TR－H－081

Time-Domain Simulation of Sound Production in the Brass Instrument

Seiji Adachi

1994. 6. 14

ATR人間情報通信研究所

〒619-02 京都府相楽郡精華町光台2-2　☎07749-5-1011

ATR Human Information Processing Research Laboratories

2-2, Hikaridai, Seika-cho, Soraku-gun, Kyoto 619-02 Japan

Telephone: +81-7749-5-1011
Facsimile: +81-7749-5-1008

Time-Domain Simulation of Sound Production in the Brass Instrument

Seiji Adachi

ATR Human Information Processing Research Laboratories,
2-2, Hikaridai, Seika-cho, Soraku-gun, Kyoto 619-02 Japan
E-mail: adachi@hip.atr.co.jp

Sound production in brass instruments is formulated physically with two different models of lip vibration: the "perpendicular" model, where lips strike laterally to the direction of the air flow, and the "swinging door" model, where lips execute an outwardly rolling motion. This formulation is used to carry out time-domain simulation, which indicates that self-excitation of the brass instrument is possible with both of these lip models. Changing the lip resonance frequency provides sustained oscillation at the first through eighth air column resonance modes, which correspond to the musical tones in the harmonic series played on the brass instrument without valve manipulation. Oscillation probably also occurred at higher modes, but that region was not investigated. The harmonic structure of the simulated sound varies according to the pitch and sound level, as is the case in the sound produced by actual brass instruments. Unusual regimes of oscillation are also obtained: the pedal tone, whose fundamental does not participate in its sound production; a tone octave below the third impedance peak, whose odd harmonics do not contribute to the regime of oscillation; and, a multiphonic, which is an oscillation perceived as having two fundamentals simultaneously.

PACS numbers: 43.75.Fg

INTRODUCTION

The aim of this paper is to show the possibilities of physical modeling for synthesizing the sound of brass instruments. Woodwind and brass instruments can be considered nonlinear oscillation systems with delayed feedback. If we adequately model the sound production of these systems and then calculate the derived equations numerically, it would be possible, in principle, to obtain all the sounds produced by the instruments. The clarinet is one of the most extensively studied wind instruments[1–5]. Schumacher[6,7] has derived equations that describe the sound production system of the clarinet to obtain waveforms of the various sounds that closely match those observed experimentally.

Schumacher's equations set a good precedent for modeling the brass instruments, but there are several differences between the sound production systems of the reed-driven woodwind instruments and the lip-driven brass instruments. On the woodwind instruments, the reed resonance frequency, which is controlled by the player's embouchure, is always much higher (for the clarinet reed, it's in the range of 2-3 kHz) than the sound frequencies. It may affect the register change and the timbre of sound, but it does not vary sound pitch. Instead, pitch is selected by the change in the acoustical characteristics of the air column, which is managed by the tonehole system. On the brass instruments, the lip-reed resonance frequency is about the same as the sound frequency. The player controls the lip-reed resonance frequency through the embouchure so that a desired pitch is selected from the harmonic series that the air column of the brass instrument provides. These distinctive features in the brass instrument system make the oscillation of the brass sound differ from that of the woodwind instrument's sound. To model the brass instrument system, it's necessary to give attention to these features, in addition to formulating the lip vibration model and calculating the acoustic characteristics of the air column.

Compared with the studies on the clarinet sound simulation, there seems to be scant published treatment of brass instrument simulation using physical modeling. Recently, Keefe[8] used physical modeling to confirm oscillation conditions derived from theoretical considerations for both woodwind and brass instruments. He treats both instruments in a unified manner with simplified acoustic characteristics of the air column, but the obtained waveforms for brass sound do not closely simulate the actual ones. Furthermore, that study did not investigate pitch selection with the adjustment of the lip resonance frequency. This may imply the necessity to develop a more appropriate formulation to deal with brass instruments. This paper presents an air flow model and lip vibration models that are especially devised for brass instruments. We have also replicated and applied the acoustic characteristics of the air column calculated from the shape of an actual trumpet.

Sounds produced by actual musical instruments have the following properties: 1) sound spectra, which provide the timbre of steady portions of musical sounds, vary according to pitch and sound level; 2) the waveforms of musical sounds are not perfectly periodic, even in their steady portions; 3) instead, they include fluctuations or deviations from the periodicity due to player effects such as vibrato and unevenness of blowing pressure. These properties are the main factors that allow musical sounds to be perceived as natural.

In the synthesis of high quality musical sounds, physical modeling has advantages over such conventional methods as additive synthesis, FM (frequency modulation) and the sampling method. Physical modeling, which takes account of the nonlinearity, has a mechanism in nature that alters the harmonic contents of produced sounds according to pitch and sound

Fig. 1

level. In the conventional methods, harmonic variation should ideally be reproduced for each pitch and sound level[9]. This is, however, not fully realized within the hardware's limited memory capacity. Sound fluctuations are also easily obtained in physical modeling. They can be generated by modulating a few parameters such as blowing pressure, and the results would be natural. On the other hand, the conventional methods produce somewhat artificial fluctuation results because they lack physical constraints. Moreover, transient waveforms, including the attack and decay portions of musical sounds, can be naturally produced with the use of time-domain simulation in physical modeling. This is also an important factor for obtaining realistic simulation, although it is not discussed here.

There is a fairly standard theory of sound production for the wind instruments[10]. According to the theory, the whole sound production system is divided into two elements: the generator and the resonator. For the brass instrument, the generator means the lips put to the mouthpiece, vibrating and regulating the air flowing into the instrument. The lip vibration can be modeled by a harmonic oscillator in the simplest case. The resonator, which is an air column confined in the instrument, can also be treated as a linear system. Contrary to the function of each of the elements, the interaction between them is nonlinear due to the fluid dynamical effect of air flow through the lip aperture. When blowing pressure is applied, lips start their motion. At the same time, air flow regulated by the lip motion makes an acoustical disturbance in the mouthpiece. The disturbance, after circulating through the instrument, returns to the mouthpiece and affects lip motion. If the lip vibration and the feedback of the disturbance are in phase, the oscillation grows or maintains.

For modeling lip vibration on an oscillator having a few degrees of freedom, the direction of the vibration must first be considered. Unlike the mechanical cane reeds of woodwind instruments, which have definite constraints on their directions of motion, biological lips deform quite unrestrictively as a lip-reed put to the mouthpiece. This means the directions of the modeled vibration are ambiguous. For this reason, there are several lip vibration models, even if each lip is considered a one-dimensional harmonic oscillator. Let us consider a pressure-controlled valve in an acoustic tube in general. Fletcher[11] classified the valve configurations into three different types (Fig. 1). In type (a), which is described as the "striking outwards" model, the valve opens further in increments of blowing pressure, while in type (b), described as the "striking inwards" model, the valve closes. In type (c), called the "perpendicular" model, Bernoulli pressure tends to close the valve. The "striking inwards" model describes the reed vibration of the woodwind instrument. Although the lip vibration of the brass instrument should be classified as type (a) or type (c), it is not yet clear which model better approximates the real lip vibration. In reality, it may not be appropriate to apply only one of these models to all of the produced sounds having different pitches and levels. There is also said to be wide variation in playing technique. In this paper, we carry out simulation with two lip vibration models, based on the valve characteristics in (a) and (c), in order to find the difference between their performances.

Sounds with aperiodic waveforms are sometime produced in this simulation, even if the system's parameters are all fixed. Their aperiodicity is not so large that their pitch sensations failed, but large enough to make their timbre somewhat impure. Such aperiodicity should be distinguished from the fluctuation in musical sounds blown by human players, as mentioned before. The cause or mechanism of producing aperiodic waveforms is in the nonlinearity of the sound production system itself. Although it is uncertain that aperiodic waveforms are observed in sounds played on actual musical instruments, there is the possibility that aperiodicity is a key factor that allows musical sounds to be perceived as natural. If this is the case, physical modeling excels as a method of synthesizing musical sounds.

I. FORMULATION

Sound production in brass instruments can be described as having the following three variables: mouthpiece sound pressure $p(t)$, air volume velocity $U(t)$ flowing through the lip orifice into the mouthpiece, and the area of the lip orifice $S_{\rm lip}$. They are used to satisfy the following three equations: 1) an equation governing air flow through the lip orifice; 2) an equation of lip motion; and, 3) an integral equation representing feedback from the instrument. These equations are derived in the following subsections.

A. Air flow dynamics

The mouth, lips and mouthpiece are schematically depicted from left to right in Fig. 2. Air flow is assumed to be one-dimensional. Contraction and expansion of the air flow occur in the upstream and downstream regions of the lips, respectively[12]. We apply energy conservation law to the flow in the contraction region, which becomes

$$p_0 - p_{\rm lip} = \frac{1}{2}\rho\left(\frac{U}{S_{\rm lip}}\right)^2 + \frac{\rho d}{S_{\rm lip}}\frac{\partial U}{\partial t}, \tag{1}$$

where p_0 is blowing pressure, $p_{\rm lip}$ pressure in the lip orifice, ρ average air density, and d thickness of the lips. In the expansion region, it is uncertain whether laminar flow is realized due to the small constriction of the lip orifice. Therefore, we consider momentum of the flow in this region instead of energy. The momentum conservation is given by

$$p_{\rm lip} - p = -\rho U^2\left(\frac{1}{S_{\rm cup}S_{\rm lip}} - \frac{1}{S_{\rm cup}^2}\right), \tag{2}$$

with $S_{\rm cup}$ as the cross-sectional area of the mouthpiece entryway. Omitted here is the inertia term of the air flow. Eq. (1) and (2) represent the nonlinear dependence between the three variables $p(t)$, $U(t)$ and $S_{\rm lip}$.

B. Modeling of lip vibration

The most proper way to deal with soft tissues such as lips would seem to be to regard them as continua with distributed mass and stiffness. However, stroboscopic measurements by Martin[13] and Hall[14] of player's lips while blowing instruments show that they oscillate in

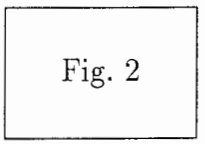

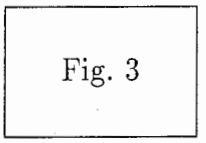

a lump. This implies that the situation, where lip vibration is modeled by a single oscillator as a first approximation, is not far from the actual one. One may consider the nonlinear behavior of the restoring force, but for simplicity, the force is assumed to satisfy Fuch's law. Accordingly, vibration amplitudes of the upper and lower lips are also assumed to be the same, although some difference is observed.

Other findings of Martin's observations are as follows: the displacement of the lip orifice is almost sinusoidal; the lips close once every cycle but closing time is very small compared to the period of oscillation; and the amplitude of the vibration tends to decrease as the frequency increases. These characteristics must be realized in the simulation.

As mentioned in the introduction, the direction of lip motion is a central question for physical modeling of brass instruments. Since Helmholtz[15] classified lip vibration into the model of "striking outwards" (Fig. 1 (a)), this model has been widely used to describe sound production of brass instruments without any experimental confirmation[16]. Saneyoshi et al.[17] questioned this understanding and raised the possibility that some oscillations can be better modeled by the "perpendicular" model. Following this, Yoshikawa[18,19] carried out simultaneous measurements of mouthpiece pressure and lip vibration. His measurements show that both of the states of oscillation supporting the "striking outwards" and the "perpendicular" models are realized. Based on these observations, we used the two lip vibration models shown in Fig. 3.

In the first model (Fig. 3 (a)), lip motion is restricted to only the direction perpendicular to air flow. We call this the "perpendicular" model as in Fig. 1 (c). The same restriction is also used in the one-mass[20] and two-mass[12] models of vocal fold vibration for speech synthesis. The lip orifice is assumed to have a rectangular shape with lip breadth b. Let lip mass be m, stiffness k, quality factor Q. Then the dynamics of lip displacement x are given by the following equation of motion,

$$m\frac{d^2x}{dt^2} = -\frac{\sqrt{mk}}{Q}\frac{dx}{dt} + bdp_{\mathrm{lip}} - kx, \tag{3}$$

where the first, second and third terms in the right hand side represent damping force, external force due to the Bernoulli effect and restoring force, respectively. The cross-sectional area of the lip orifice is given by $S_{\mathrm{lip}} = \max\{b(2x + x_0), 0\}$ with the equilibrium lip opening length x_0. During closure of the lips, that is when $x < -x_0/2$, an additional restoring force proportional to $2x + x_0$ is supplied.

Table I

Fig. 3 (b) illustrates the second model, called the "swinging-door" model, where the lips execute a rolling motion in the mouthpiece cup. This results in the outwardly striking valve model shown in Fig. 1 (a) because the lips are driven by the difference between blowing pressure p_0 and mouthpiece pressure p. In this model, it is convenient to use angle θ of each lip to a normal plane of the air flow direction as a dynamical variable representing lip displacement. The equation of motion is written as

$$ml\frac{d^2\theta}{dt^2} = -\frac{\sqrt{mk}}{Q}l\frac{d\theta}{dt} + \frac{1}{2}bl(p_0 - p) + bdp_{\rm lip}\sin\theta - kl(\theta - \theta_0), \tag{4}$$

where l is lip length from the mouthpiece rim to the tip of the lip and θ_0 equilibrium lip angle. The first through the last terms in the right hand side represent damping force, external force generated by the pressure difference, external force due to the Bernoulli effect and restoring force, respectively. When lip angle θ is less than the lip closing angle $\theta_{\rm cl}$, contact force proportional to $\theta - \theta_{\rm cl}$ acts on both lips. The cross-sectional area of the lip orifice is given by $S_{\rm lip} = \max\{2b\,l(\cos\theta_{\rm cl} - \cos\theta), 0\}$. Unlike with the "perpendicular" model, this model requires consideration of volume flow rate $bl^2d\theta/dt$ produced by the lip motion in addition to the aerodynamical volume flow rate examined in the previous subsection.

Adjusting the lip resonance frequency, the player selects pitches of musical sounds assigned to the air column resonance modes of the brass instrument. Elliot and Bowsher[21] deduced dependence of lip mass m on the lip resonance frequency $f_{\rm lip}$ from their measurements of average volume flows while sounds are produced at various pitches. Following their results, we assume that m is inversely proportional to $f_{\rm lip}$. Accordingly, the behavior of stiffness k becomes $k \propto f_{\rm lip}$ because $f_{\rm lip} = \sqrt{k/m}/2\pi$. Lip and other parameters for our simulations are shown in Table I.

C. Input impedance and reflection function

The acoustic properties of the air column are characterized by input impedance $Z_{\rm in}(f)$, which is the ratio of mouthpiece pressure to volume velocity with frequency f. This quantity $Z_{\rm in}(f)$ is compared to the characteristic wave impedance $Z_{\rm c} = \rho c/S_{\rm cup}$ of an infinite cylindrical tube having the same area $S_{\rm cup}$ as the mouthpiece entryway. The reflection function $r(t)$ is defined by the inverse Fourier transformation of the following ratio

$$\hat{r}(f) = \frac{Z_{\rm in}(f) - Z_{\rm c}}{Z_{\rm in}(f) + Z_{\rm c}}. \tag{5}$$

Physically, $r(t)$ represents pressure waveform reflected back to the mouthpiece after the incidence of a pressure impulse to the instrument at $t = 0$. Using the reflection function $r(t)$, Schumacher[7] developed an effective method to calculate the acoustic response of the air column. Compared to other methods that use the Green function, defined by the Fourier

Fig. 4

Table II

transform of Z_{in}, an enormous amount of calculation time is saved. With the reflection function, mouthpiece pressure $p(t)$ at the present time t is calculated from the present volume velocity $U(t)$ and their past data $p(t-s)$ and $U(t-s)$ for $s > 0$ as follows,

$$p(t) = Z_{\text{c}}U(t) + \int_0^\infty ds\, r(s)\,(Z_{\text{c}}U(t-s) + p(t-s))\,. \tag{6}$$

We also employ this equation in our time-domain simulation.

To obtain realistic brass sounds in physical modeling, it is necessary to pay as much attention to the acoustic characteristics of the air column as to the other components. There are two types of methods to obtain an appropriate input impedance Z_{in} that precisely represents the air column characteristics. The first one is measuring this quantity Z_{in} directly on an existing instrument[22,23]. The other is invoking knowledge of acoustics[24,25]. In the latter type, the instrument bore is first divided into a series of small sections so that a simple acoustic element can be substituted for each section. Then, the product of transfer matrices for those sections is calculated. We used such a method developed by Caussé et al.[24] that employs truncated cones as the acoustic elements. This calculation considers visco-thermal loss, i.e. loss due to the friction and thermal exchange between the air and the wall of the instrument. Radiation loss is calculated here on the assumption that the spherical wave is radiated to the ambient from the bell of the instrument.

We measured the dimensions of a Yamaha B$^\flat$ trumpet model YTR-2320E (student model) and used them for the Z_{in} calculation. The magnitude and phase of Z_{in} are illustrated in Fig. 4. In Table II, the magnitudes and frequencies of the input impedance peaks are listed along with the intervals between the frequencies. Except for the first peak, they are all at nearly equal intervals. This shows that the instrument is almost in tune because the first resonance mode is not ordinarily used for blowing brass instruments. As for magnitude, the peaks with frequencies of about 500 Hz are enhanced by the resonance in the mouthpiece cup. The phase of Z_{in} is shifted toward negative values at the higher side of the mouthpiece cup's resonance frequency. This behavior of the input impedance due to the mouthpiece cup resonance accurately characterizes the air column of the brass instruments.

From the obtained input impedance Z_{in}, it is possible, by definition, to calculate the reflection function $r(t)$ by carrying out the inverse Fourier transform of Eq. (5). However, there arises a difficulty with the practical numerical calculation if abrupt reflection from the mouthpiece entryway yields discontinuity in $r(t)$ at $t = 0$. This happens whenever the cross-sectional area of the mouthpiece entryway varies along the airflow direction as in the case of

Fig. 5

the brass instruments. In the numerical calculation, such abrupt reflection makes the value of $r(t)$ at $t < 0$ nonzero, therefore breaking the causality. This is due to the cut-off frequency or the sampling frequency pursued to the discrete calculation. In this case, Eq. (6) cannot be applied to the simulation exactly as it stands. To make it applicable, we reconstructed a causal reflection function $r^{\mathrm{c}}(t)$ from the even component of the original $r(t)$, which seems not affected by the cut-off frequency because of its continuity at $t = 0$ as follows,

$$r^{\mathrm{c}}(t) = \begin{cases} r(t) + r(-t) & \text{for } t \geq 0, \\ 0 & \text{for } t < 0. \end{cases} \tag{7}$$

To assure the validity of this procedure, it has been confirmed that Eq. (6) with this causal reflection function $r^{\mathrm{c}}(t)$ simulates a ratio of generated pressure p to input volume velocity U, reproducing almost the same input impedance Z_{in}. Fig. 5 shows the appearance of the reflection function $r^{\mathrm{c}}(t)$. The reflection from the instrument's bell appears as a dip near $t = 8$ msec. in $r^{\mathrm{c}}(t)$. Subsequent dips exponentially fading out manifest multiple reflections that travel more than one time between the bell and the mouthpiece. A sharp peak just after $t = 0$ and a valley following the peak correspond to reflections from the mouthpiece cup and the tapered section (i.e. the mouthpiece backbore to the leader pipe), respectively.

D. Linear theory of oscillation

In the previous subsections, the sound production system of the brass instrument was formulated with two linear elements, the lip dynamics and the air column response, and their nonlinear interaction governing air flow through the lip orifice. To gain insight into this system before considering the simulations, this subsection investigates conditions under which self-oscillation is maintained within a linear theory when the amplitude of oscillation is small.

First, consider time-averaged or D.C. components of the variables, p_{lip}, U and S_{lip}, which are expressed with barred symbols, $\bar{p}_{\mathrm{lip}}$, $\bar{U}$ and $\bar{S}_{\mathrm{lip}}$, respectively. The mouthpiece pressure p does not have a D.C. component[26]. Hereafter in this subsection, the original notation, p_{lip}, U and S_{lip}, expresses the time-varying or A.C. components. The D.C. components satisfy the following stationary conditions,

$$p_0 - \bar{p}_{\mathrm{lip}} = \frac{1}{2}\rho \left(\frac{\bar{U}}{\bar{S}_{\mathrm{lip}}} \right)^2, \tag{8}$$

$$\bar{p}_{\mathrm{lip}} = -\rho \bar{U}^2 \left(\frac{1}{S_{\mathrm{cup}} \bar{S}_{\mathrm{lip}}} - \frac{1}{S_{\mathrm{cup}}^2} \right), \tag{9}$$

which are derived from the air flow equations (1) and (2). The values of $\bar{p}_{\mathrm{lip}}$, $\bar{U}$ and $\bar{S}_{\mathrm{lip}}$ are determined by Eq. (8), (9) and an equilibrium condition that represents a balance between

Fig. 6

the restoring and external forces acting on lips. Supposing $\bar{S}_{\rm lip} \ll S_{\rm cup}$, we have

$$\bar{p}_{\rm lip} = 0, \tag{10}$$

$$\bar{U} = \sqrt{\frac{2p_0}{\rho}}\bar{S}_{\rm lip}, \tag{11}$$

$$\bar{S}_{\rm lip} = \begin{cases} bx_0, & \text{“perpendicular” model} \\ 2bl\left(\cos\theta_{\rm cl} - \cos\bar{\theta}\right), \quad \bar{\theta} \equiv \theta_0 + \dfrac{bp_0}{2k}, & \text{“swinging-door” model.} \end{cases} \tag{12}$$

Eqs. (1) and (2), governing the nonlinear air flow dynamics, are linearized as

$$\left(1 + d\frac{\bar{S}_{\rm lip}}{\bar{U}}\frac{d}{dt}\right)\frac{U}{\bar{U}} = -\frac{p_{\rm lip}}{2p_0} + \frac{S_{\rm lip}}{\bar{S}_{\rm lip}}, \tag{13}$$

$$p = p_{\rm lip}, \tag{14}$$

where $\bar{S}_{\rm lip} \ll S_{\rm cup}$. In the ordinary range of brass instrument sound frequencies. the inertia of air flowing through the lip orifice can be neglected. Therefore, we drop the second term in parentheses on the left hand side of Eq. (13) from consideration. Eqs. (13) and (14) show that air flow rate increases as the area of the lip orifice increases, and that air flow rate decreases as the mouthpiece pressure increases.

Lip mobility G is defined here by $G = S_{\rm lip}(f)/p(f)$, where $S_{\rm lip}(f)$ and $p(f)$ denote Fourier components of $S_{\rm lip}$ and p at frequency f, respectively. From Eq. (3) and (4), lip mobility G becomes

$$G(f) = \begin{cases} \dfrac{2b^2d}{k}\Lambda\left(\dfrac{f}{f_{\rm lip}}\right), & \text{“perpendicular” model} \\ -\dfrac{b^2l}{k}\sin\bar{\theta}\left(1 - 2\dfrac{d}{l}\sin\bar{\theta}\right)\Lambda\left(\dfrac{f}{f_{\rm lip}}\right), & \text{“swinging-door” model} \end{cases} \tag{15}$$

where the function $\Lambda(\Omega)$ is defined by

$$\Lambda(\Omega) = \frac{1}{1 - \Omega^2 + i\dfrac{\Omega}{Q}}. \tag{16}$$

The appearance of $\Lambda(\Omega)$ is denoted in Fig. 6. Eq. (15) shows that $|G(f)|$ takes its maximum near the lip resonance frequency $f_{\rm lip}$, and that $\angle G(f)$ exhibits π decrease from the lower side to the higher side of $f_{\rm lip}$. A model difference appears on the sign of $\angle G$: for the “perpendicular” model, $\angle G < 0$ holds; whereas for the “swinging-door” model. $\angle G > 0$ is satisfied.

Substituting definitions of lip mobility G and input impedance Z_{in} into the linearized air flow equations (13) and (14), we have the stationary self-oscillation condition as follows,

$$K(f) \equiv \sqrt{\frac{2p_0}{\rho}}\tilde{G}(f)Z_{\text{in}}(f) = 1, \tag{17}$$

where $\tilde{G}$ is defined by

$$\tilde{G} = G - \frac{\bar{S}_{\text{lip}}}{2p_0}. \tag{18}$$

Note here that the magnitude of $\tilde{G}$ is also maximized near the lip resonance frequency and that the angle of $\tilde{G}$ has the same sign as the angle of G. Oscillation grows under the condition that there exists a frequency f such that $K(f)$ is real and larger than 1. The magnitude condition, $K(f) > 1$, requires that both magnitudes of Z_{in} and $\tilde{G}$ are large. This indicates that the oscillation most likely to be generated has a frequency f is near one of the air column resonance frequencies as well as near the lip resonance frequency. The phase condition is written as $\angle\tilde{G} + \angle Z_{\text{in}} = 0$. Because of the model dependence of the sign of $\angle\tilde{G}$, this is satisfied only if $\angle Z_{\text{in}}$ is positive for oscillation in the "perpendicular" model and only if it is negative for oscillation in the "swinging-door" model. In the ordinary range of the brass instrument's sound frequency, the phase angle of Z_{in} is positive on the lower frequency side of the input impedance peaks and negative on the higher frequency side (Fig. 4). Therefore, it can be concluded that the "perpendicular" model operates on the lower frequency side of the input impedance peaks and the "swinging-door" model operates on the higher side.

II. SIMULATION RESULTS

A. Mode selection

Difference equations, derived from the differential equations by means of the forward Euler method with 8 kHz sampling frequency, are used in time-domain simulation. Blowing pressure for the moderate sound level (mf) is set at 2.0, 2.0, 2.5, 3.0, 3.5, 4.0, 4.0, 4.0 kPa for the first through eighth air column resonance modes, respectively. Lip opening length x_0, and lip angle θ_0 at equilibrium are adjusted so that the following conditions are satisfied: 1) the lips do not come into contact with each other or only have contact in a much shorter time than the oscillation period; and 2) the maximum amplitude of oscillation is obtained.

The mode selection was investigated first. By changing the lip resonance frequency from 60 Hz to 800 Hz at intervals of 20 Hz, we obtained frequencies of self-excited sound (Fig. 7). It was found that, for both lip models, sound production is possible at the first through eighth air column resonance modes. The higher modes are probably also excited, though that region was not investigated. As derived in subsection I-D, sounds are produced on the lower frequency side of the input impedance peaks for the "perpendicular" model and on the higher side for the "swinging-door" model. From each lip vibration model's ascending series of pitch, a harmonic series can be constructed in tune by selecting the sound with an appropriate pitch from each resonance mode. The absolute pitch of sounds in the "swinging door" model is about a half note higher than that of sounds in the "perpendicular" model, which accords with B$^\flat$ trumpet pitch. This does not imply inferiority of the "swinging door" model because higher pitch can be lowered by withdrawing the tuning slide.

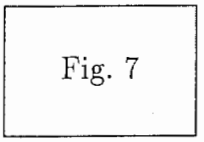

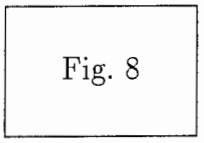

Let us examine mode selection between the second and third resonance modes in detail. The magnitude and phase angle of $K(f)$ defined by Eq. (17) are plotted in Fig. 8: (a) $f_{\mathrm{lip}} = 260$ Hz, (b) $f_{\mathrm{lip}} = 400$ Hz for the "perpendicular" model, and (c) $f_{\mathrm{lip}} = 160$ Hz, (d) $f_{\mathrm{lip}} = 240$ Hz for the "swinging-door" model. In (a) $f_{\mathrm{lip}} = 260$ Hz, there is a frequency that satisfies both the magnitude and phase conditions only in the second resonance mode. In (b) $f_{\mathrm{lip}} = 400$ Hz, there is such a frequency only in the third mode. These accord with the simulation results showing that the second and third modes are excited for $f_{\mathrm{lip}} = 260$ Hz and 400 Hz, respectively. This examination is also valid for the "swinging-door" model. For $f_{\mathrm{lip}} = 160$ Hz ((c)), only the second mode satisfies the oscillation conditions and is excited in the simulation. Likewise, for $f_{\mathrm{lip}} = 240$ Hz ((d)), the third mode selected from the conditions is realized in the simulation.

As typical results obtained in the simulation, we examine oscillation in the second resonance mode, whose waveforms are shown in Fig. 9. In both lip vibration models, the waveform of S_{lip} is almost sinusoidal, whereas those of p and U contain rich higher harmonics. This is analogous to the oscillation behavior observed in the sound production in the actual brass instruments. The phase relationships between the variables p, U and S_{lip} provide the most significant difference between the lip vibration models. Apparently, the phase of p, $\angle p$, is advanced to that of U, $\angle U$ for the "perpendicular" model, whereas $\angle p$ is retarded to $\angle U$ for the "swinging-door" model. More precisely, $\angle p - \angle U = 76.3°$ holds for the oscillation in the "perpendicular" model, whereas $\angle p - \angle U = -44.1°$ is obtained for the oscillation in the "swinging-door" model. The phase condition $\angle \tilde{G} + \angle Z_{\mathrm{in}} = 0$ derived from a linear oscillation theory is not satisfied: $\angle \tilde{G} + \angle Z_{\mathrm{in}} = 10.6°$ for the oscillation in the "perpendicular" model; and $\angle \tilde{G} + \angle Z_{\mathrm{in}} = -26.7°$ for the oscillation in the "swinging-door" model. This implies that oscillation at the moderate sound level can no longer be considered infinitesimal.

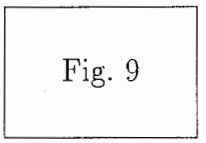

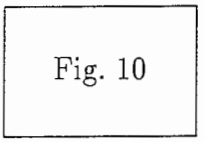

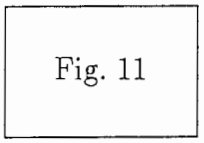

B. Pitch and strength variations

We compare the pressure waveforms of oscillation at the second through sixth resonance modes (Fig. 10). In both lip vibration models, sounds with lower pitch have characteristic waveforms with plateaus and downward spikes, which gradually become sinusoidal waveforms at higher pitches. This successfully simulates the change in the observed brass sound[27]. The log amplitudes of the harmonics of oscillation for the second, fourth and sixth modes are plotted against the harmonic number in Fig. 11. This shows the same tendency that higher harmonics disappear as the pitch increases, except for the transition between the second and fourth modes in the "swinging-door" model. This may be because the amplitude of the second mode oscillation is not as large as the other amplitudes. It has not been shown that the decrease in log amplitude is constant with the harmonic number, although this is predicted by a theoretical consideration and observed in actual brass sound[21]. Along with the overall deficiency of harmonics, this may suggest the necessity to search for the parameter space of the sound production system over a broader range.

Our simulation also provides change in harmonic structure against sound strength. The pressure waveforms of oscillation at the second resonance mode on various sound levels are depicted in Fig. 12. Blowing pressures for the lower sound level (pp), moderate level (mf) and higher level (ff) are supplied at 0.5, 2.0 and 6.0 kPa, respectively. As sound strength increases, the pressure waveform tends to have rich harmonics. The same tendency is also shown in Fig. 13, where the decline of the log plot of harmonic amplitudes becomes less at higher sound strength.

C. Unusual regimes of oscillation

Some oscillations are excited considerably off the frequencies of impedance peaks, unlike the usual oscillations in the resonance modes. In Fig. 7, such oscillation in the "perpendicular"

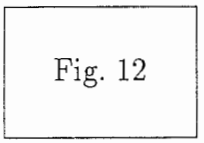

Fig. 13

Table III

model is found between the first and second resonance modes. It is identified with what is called "loose-lipping" tone[28], which has a pitch octave below the third impedance peak. In the "swinging-door" model, oscillation in the first mode has noticeably higher frequency than that of the first impedance peak. It is considered the pedal tone, whose pitch is an octave below the second impedance peak.

Let us compare these two unusual regimes of oscillation with a usual one, e.g. oscillation with the "perpendicular" model in the second resonance mode. Table III lists the values of input impedance of the harmonic frequencies of oscillations. It was found that the second, third, fifth and sixth harmonics mainly contribute to the regime of oscillation of the "loose-lipping" tone, and that the second, fourth and sixth harmonics mainly contribute to the regime of oscillation of the pedal tone. In both cases, the values of Z_{in} of the fundamental frequencies are very small. On the other hand, all of the harmonics, including the fundamental, equally contribute to the usual regime of oscillation.

The "loose-lipping" tone is especially extraordinary. The value of Z_{in} of the fundamental frequency is so small that no f satisfies the oscillation conditions for $K(f)$ derived in subsection I-D. This means that the linear theory, where only the fundamental is taken into consideration, cannot prove the existence of this self-oscillation. Rather, we must consider the cause the mode coupling due to the nonlinearity in the sound production.

D. Aperiodic oscillation

Generally, the simulation system produces periodic oscillation, one example of which has the waveform and spectrum shown in Fig. 14 (a). However, in some cases we obtain aperiodic oscillation, such as shown in Fig. 14 (b). Aperiodicity is not so large that the pitch sensation fails, but it does make the sound impure to some extent. Both the nonlinearity of the air flow dynamics and the nonlinearity caused by the lip collision must participate in the production of aperiodic oscillation, although this mechanism is not investigated here.

Multiphonics are the regimes of oscillation that are perceived as having two separate pitches sounding simultaneously. It is said that multiphonics in the brass instrument sometime happen unintentionally as the result of a novice players' misblow. Fig. 14 (c) shows a multiphonic obtained in the simulation, which provides two fundamentals with a broadband spectrum. The frequencies of these fundamentals indicate that the third and fourth air column resonance modes are excited in this oscillation. To obtain this, the lip resonance

Fig. 14

frequency is set at 280 Hz, which is in the middle of the lip resonance frequencies, to produce third and fourth resonance mode oscillation in the "swinging-door" model.

In a system with delayed feedback, such as the sound production system investigated here, there is sometimes hysteresis, which is a phenomenon where the state of oscillation is selected not only by the parameters but also by the previous state of oscillation. For an artificial blowing system of the clarinet[29], for example, hysteretic transition of the oscillation states was fully investigated. In our simulation of the brass sound production system, hysteresis is also observed. With the same parameters, $p_0 = 2.5$ kPa, $\theta_0 = 38.0°$ and $f_{\mathrm{lip}} = 280$ Hz, as those for the multiphonic mentioned in the previous paragraph, periodic oscillation in the fourth mode can also be produced depending on the previous state of oscillation.

III. CONCLUSIONS

The sound production system of the brass instruments is formulated with a physical model that consists of the air flow dynamics, two lip vibration models (i.e. the "perpendicular" model and the"swinging-door" model), and the realistic air column response calculated from the shape of an actual $B^{\flat}$ trumpet. By adopting both of the lip vibration models, the whole system successfully simulates brass sounds having various pitches and sound levels. Simulation results are summarized as follows:

1) Changing lip resonance frequency reproduces sustained oscillation in the first through eighth air column resonance modes, i.e. the musical sounds in the harmonic series of the brass instruments.

2) The spectrum of the simulated sound varies according to the pitch and sound level, as found in the actual brass instrument sound.

3) The pedal tone and so-called "loose-lipping" tone are excited off the input impedance peaks. These oscillations are unusual because the air column response of the instrument supports the regime of oscillation through the mode coupling between the fundamental and the other harmonics, rather than directly supporting the fundamental itself.

4) Our sound production system also produced aperiodic oscillation, whose aperiodicity is not so large as to cause the pitch sensation to fail, but large enough to be perceived as somewhat impure. This is distinguished from oscillation fluctuating with vibrato or uneven blowing because the system's parameters were all fixed during simulation. The nonlinearity in the system is considered the cause of such aperiodic oscillation. There is the possibility that this aperiodicity also allows musical sounds to be perceived as natural as well as fluctuations due to player effects, although this is not observed in the sound played on actual musical instruments, so far.

From our simulation results, it is not possible to conclude which lip vibration model is suitable for the brass instrument sound production because the simulation behaviors of these models are similar, except for the absolute pitch difference. Recent measurements[30] of the phase difference between the lip vibration and the mouthpiece pressure seem to show that oscillation supporting the "striking outwards" model are excited in a couple of the lowest air column resonance modes and that oscillation supporting the "perpendicular" model are generated in the higher modes. If this transition of lip vibration states occurs in reality, our lip vibration models are both unsatisfactory and a more precise model that describes this transition is needed. This may be a two-dimensional model that allows lips to vibrate in both parallel and perpendicular directions to the air flow.

Transient behavior such as the attack and decay portions of musical sounds, which is not investigated in this paper, is one of the factors that characterize sound of each musical instrument. Physical modeling can also simulate transient waveforms. To do this, it is necessary to determine time dependences of the system's parameters. In a realistic situation, the player skillfully controls the parameters such as blowing pressure so as to make the produced sound expressive. In this simulation, all of the parameters are set at constant values while calculating sound waveforms. Consequently, the periods of the simulated sound's attack portions, which vary a few msec. to a few sec., are sometimes too long.

To improve this simulation of the brass instrument, apart from the issues mentioned in the previous two paragraphs, future study should consider wall vibration of the instrument, the player's respiratory system[31] and models of two-dimensional air flow.

ACKNOWLEDGEMENTS

The author wishes to thank Mr. H. Ohtsuki and Mr. H. Tamagawa for useful discussions and programming assistance. Special thanks to Dr. M. Sato for careful reading of this manuscript.

REFERENCES

[1] J. Backus, "Vibrations of the Reed and Air Column in the Clarinet," J. Acoust. Soc. Am. **33** (6), 806-809 (1961).

[2] J. Backus, "Small-Vibration Theory of the Clarinet," J. Acoust. Soc. Am. **35**, 305-313 (1963).

[3] W. E. Worman, "Self-Sustained Nonlinear Oscillations of Medium Amplitude in Clarinet-like Systems," Ph.D.Thesis, Case Western Reserve University (1971).

[4] J. Gilbert, J. Kergomard and E. Ngoya, "Calculation of the Steady-State Oscillations of a Clarinet using the Harmonic Balance Technique," J. Acoust. Soc. Am. **86** (1), 35-41 (1989).

[5] M. E. McIntyre, R. T. Schumacher and J. Woodhouse, "On the Oscillations of Musical Instruments," J. Acoust. Soc. Am. **74** (5), 1325-1344 (1983).

[6] R. T. Schumacher, "Self-Sustained Oscillations of the Clarinet: A Integral Equation Approach," Acustica **40**, 298-309 (1978).

[7] R. T. Schumacher, "*Ab Initio* Calculations of the Oscillations of a Clarinet," Acustica **48**, 71-85 (1981).

[8] D. H. Keefe, "Physical Modeling of Wind Instruments," Comput. Music J. **16** (4), 57-73 (1992).

[9] J. A. Moorer, "Signal Processing Aspects of Computer Music: A Survey," Proceedings of the IEEE **65** (8), 1108-1137 (1977).

[10] N. H. Fletcher and T. D. Rossing, *The Physics of Musical Instruments* (Springer-Verlag, New York, 1991).

[11] N. H. Fletcher, "Autonomous Vibration of Simple Pressure-Controlled Valves in Gas Flows," J. Acoust. Soc. Am. **93** (4), 2172-2180 (1993).

[12] Similar contraction and expansion of the air flow are considered in a glottal flow model in K. Ishizaka and J. L. Flanagan, "Synthesis of Voiced Sounds from a Two-Mass Model of the Vocal Cords," Bell Syst. Tech. J. **51** 1233-1268 (1972).

[13] D. W. Martin, "Lip Vibrations in a Cornet Mouthpiece," J. Acoust. Soc. Am. **13** 305-308 (1942).

[14] D. E. Hall, *Musical Acoustics* (Brooks/Cole, Pacific Grove, 1991), 2nd ed..

[15] H. L. F. Helmholtz, *On the Sensations of Tone* (Dover, New York, reprinted 1954).

[16] N. H. Fletcher, "Excitation Mechanisms in Woodwind and Brass Instruments," Acustica **43**, 63-72 (1979).

[17] J. Saneyoshi, H. Teramura and S. Yoshikawa, "Feedback Oscillations in Reed Woodwind and Brasswind Instruments," Acustica **62**, 194-210 (1987).

[18] S. Yoshikawa, "On the Modeling of Self-Oscillation in Brass Instruments," J. Acoust. Soc. Am. **84**, S161 (1988).

[19] S. Yoshikawa and G. R. Plitnik, "A Preliminary Investigation of Brass Player's Lip Behavior," J. Acoust. Soc. Jpn. (E) **14**, 449-451 (1993).

[20] J. L. Flanagan and L. L. Landgraf, "Self-Oscillating Source for Vocal-Tract Synthesizers," IEEE Trans. Audio Electroacoust. **AU-16**, 57-64 (1968).

[21] S. J. Elliott and J. M. Bowsher, "Regeneration in Brass Wind Instruments," J. Sound Vib. **83** (2), 181-217 (1982).

[22] J. Backus, "Input Impedance Curves for the Brass Instruments," J. Acoust. Soc. Am. **60** (2), 470-480 (1976).

[23] A. H. Benade, "The Physics of Brasses," Sci. Am. **299**, 24-35 (July 1973).

[24] R. Caussé, J. Kergomard and X. Lurton, "Input Impedance of Brass Musical Instruments — Comparison between Experiments and Numerical Models," J. Acoust. Soc. Am. **75** (1), 241-254 (1984).

[25] G. R. Plitnik and W. J. Strong, "Numerical Method for Calculating Input Impedance of the Oboe," J. Acoust. Soc. Am. **65** (3), 816-825 (1979).

[26] Ambient pressure is set at 0.

[27] J. Backus and T. C. Hundley, "Harmonic Generation in the Trumpet," J. Acoust. Soc. Am. **49** (2), 509-519 (1971).

[28] A. Baines, *Brass Instruments: Their History and Development* (Faber and Faber, 1976).

[29] T. Idogawa, T. Kobata, K. Komuro and M. Iwaki, "Nonlinear Vibrations in the Air Column of a Clarinet Artificially Blown," J. Acoust. Soc. Am. **93** (1), 540-551 (1993).

[30] S. Yoshikawa, "Phase Difference between the Lip Vibration and Acoustic Pressure in Brass Instrument Mouthpieces (3rd Rept.)," J. Acoust. Soc. Jpn. 2-2-16, (March 1994).

[31] S. D. Sommerfeldt and W. J. Strong, "Simulation of a Player-Clarinet System," J. Acoust. Soc. Am. **83** (5), 1908-1918 (1988).

FIGURE CAPTIONS

1. Three different configurations of a pressure-controlled valve in an acoustic tube. In each configuration, p_0 is pressure in the upstream region of the valve, i.e. blowing pressure, and p is pressure in the downstream region of the valve, i.e. mouthpiece pressure. In (a), described as the "striking outwards" model, blowing pressure p_0 tends to open the valve, whereas in (b), described as the "striking inwards" model, p_0 tends to close the valve. In (c), called the "perpendicular" model, Bernoulli pressure generated by the air flow tends to close the valve. (a) and (c) present brass instrument lip-reed models. (b) corresponds to the woodwind instrument reed vibration.

2. Schematic diagram of mouth, lips and mouthpiece. p_0, $p_{\rm lip}$ and p represent blowing pressure, pressure at the lip orifice and mouthpiece pressure, respectively. U denotes the volume velocity flowing through the lip orifice.

3. Two lip vibration models. In both models, each lip is assumed to be a harmonic oscillator with mass m, stiffness k, and quality factor Q. (a) depicts the "perpendicular" model, where lips strike laterally to the direction of the air flow. The area of the lip orifice $S_{\rm lip}$ is given by $S_{\rm lip} = \max\{b(x_0 + 2x), 0\}$ with breadth of lip orifice b, equilibrium lip opening length x_0 and lip displacement x. In the "swinging-door" model (b), lips execute an outwardly rolling motion toward the downstream of the air flow. $S_{\rm lip}$ is given by $S_{\rm lip} = \max\{2bl(\cos\theta_{\rm cl} - \cos\theta), 0\}$, where l is lip length, $\theta_{\rm cl}$ the lip closing angle and θ the lip angle.

4. The magnitude and phase angle of input impedance $Z_{\rm in}$ scaled by the characteristic wave impedance $Z_{\rm c}$, which is calculated from the shape of an actual B$^\flat$ trumpet.

5. Reflection function $r^{\rm c}(t)$. A dip near $t = 8$ msec. represents reflection from the instruments' bell. Subsequent dips damping exponentially indicate multiple reflections between the bell and the mouthpiece. An overshoot (not shown) and a valley just after $t = 0$ correspond to reflections from the mouthpiece cup and the tapered section of the instrument bore.

6. The function $\Lambda(\Omega)$, which takes the maximum absolute value Q at the normalized resonance frequency $\Omega = 1$. The phase angle of $\Lambda(\Omega)$ varies from 0 to $-\pi$ as Ω rises.

7. Behavior of the sound frequency with respect to the lip resonance frequency. In the "perpendicular" model, oscillation is realized on the lower frequency side of the input impedance peaks, while in the "swinging-door" model oscillation is on the higher frequency side.

8. The magnitude and phase angle of $K(f)$ for two different lip resonance frequencies $f_{\rm lip}$'s in each lip vibration model. (a) and (b) are calculation results for the "perpendicular" model. In (a) for $f_{\rm lip} = 260$ Hz, there exists f satisfying both conditions $K(f) \geq 1$ and $\angle K(f) = 0$ only in the second resonance mode, while in (b) for $f_{\rm lip} = 260$ Hz, such a frequency exists only at the third mode. These results correspond to the mode transition shown in the simulation. Similarly, (c) for $f_{\rm lip} = 160$ Hz and (d) for $f_{\rm lip} = 240$ Hz also show the transition between the second and the third resonance modes in the "swinging-door" model.

9. Waveforms of mouthpiece pressure p, volume flow rate U and lip displacement x or lip angle θ for each lip vibration model. x and θ show almost sinusoidal waveforms, whereas the oscillations of p and U have rich harmonics. A model difference appears in the phase difference between the oscillations of p and U. The phase of p is advanced to that of U in the "perpendicular" model and retarded to that of U in the "swinging-door" model.

10. Pressure waveforms of oscillation in the second through sixth air column resonance modes. The non-sinusoidal waveform at the lower pitch gradually disappears in the oscillation at the higher pitch.

11. Log amplitudes of Fourier components of oscillation in the second ($\bigcirc$), fourth ($\times$), and sixth ($+$) modes.

12. Pressure waveforms of the second resonance mode oscillation at the various sound levels of *pp*, *mf* and *ff*.

13. Log amplitudes of Fourier components of oscillation at sound levels *pp* ($+$), *mf* ($\bigcirc$) and *ff* ($\times$).

14. Pressure waveforms and sound spectra of three different oscillation states: (a) periodic oscillation; (b) aperiodic oscillation; (c) multiphonic.

Table I: Parameters in brass sound production system

Symbol	Parameter Name	Value
c	Speed of sound	3.4×10^2 m/s
ρ	Average air density	1.2×10^3 kg/m^3
S_{cup}	Area of mouthpiece entryway	2.3×10^{-4} m^2
b	Breadth of lip orifice	8.0×10^{-3} m
d	Thickness of lips	2.0×10^{-3} m
l	Length of lips ("swinging-door" model)	8.0×10^{-3} m
x_0	Equilibrium lip opening length ("perpendicular" model)	$2.1 \times 10^{-4} \sim 2.4 \times 10^{-3}$ m
θ_0	Equilibrium lip angle ("swinging-door" model)	$34.0 \sim 40.0°$
θ_{cl}	Lip closing angle ("swinging-door" model)	$40.0°$
Q	Lip quality factor	5.0
f_{lip}	Lip resonance frequency	$60 \sim 800$ Hz
m	Lip mass ("perpendicular" model)	$1.5/\left((2\pi)^2 f_{\text{lip}}\right)$ kg
	Lip mass ("swinging-door" model)	$0.55/\left((2\pi)^2 f_{\text{lip}}\right)$ kg
k	Stiffness of lips ("perpendicular" model)	$1.5 f_{\text{lip}}$ N/m
	Stiffness of lips ("swinging-door" model)	$0.55 f_{\text{lip}}$ N/m
p_0	Blowing pressure	$0.5 \sim 6.0$ kPa

Table II: Magnitudes and frequencies of input impedance peaks and their intervals

Mode	$\lvert Z_{\mathrm{in}}/Z_{\mathrm{c}}\rvert$	Frequency(Hz)	Interval(Hz)
1^{st} Pd	43.7	87	
2^{nd} $\mathrm{B}_3^{\flat}$	35.2	232	145
3^{rd} F_4	46.4	341	109
4^{th} $\mathrm{B}_4^{\flat}$	55.7	457	116
5^{th} D_5	48.1	572	115
6^{th} F_5	51.6	686	114
7^{th} $\mathrm{A}_5^{\flat}$	44.5	800	114
8^{th} $\mathrm{B}_5^{\flat}$	28.5	913	113

Table III: Values of input impedance $|Z_{\mathrm{in}}/Z_{\mathrm{c}}|$ of harmonic frequencies of three different types of oscillation

Type of oscillation	f_{lip} (Hz)	f (Hz)	fund.	2nd	3rd	4th	5th	6th
"Loose-lipping"	160	159	2.8	15.1	16.7	5.3	42.2	13.1
Pedal	100	121	1.2	10.9	6.7	10.5	8.7	10.4
Normal	260	217	13.1	17.9	10.5	7.7	10.5	9.6

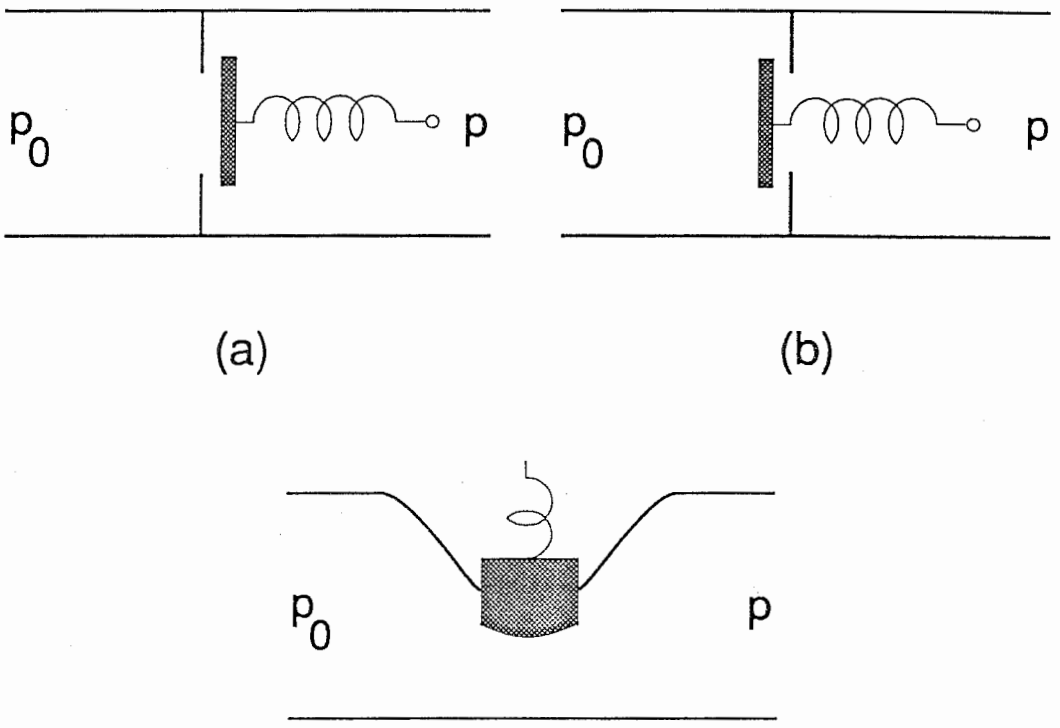

Figure 1

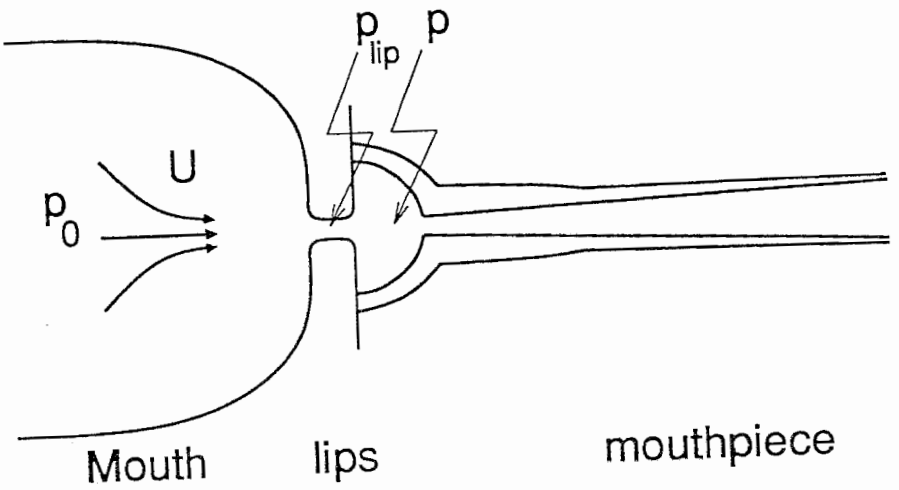

Figure 2

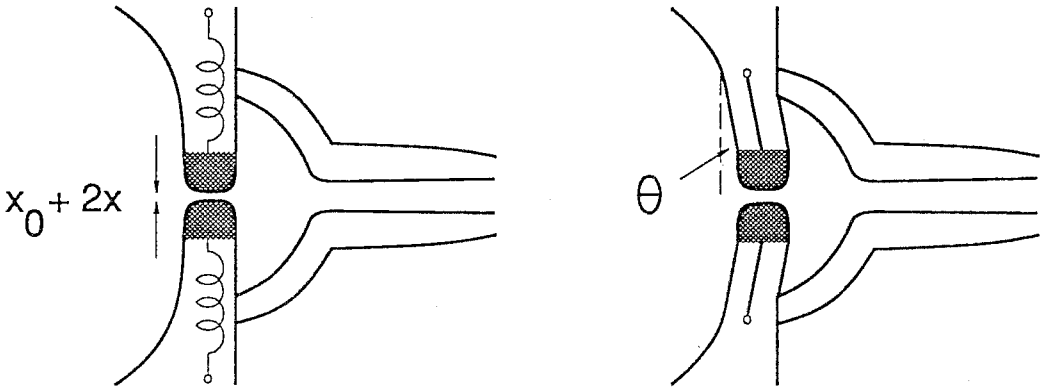

(a) (b)

Figure 3

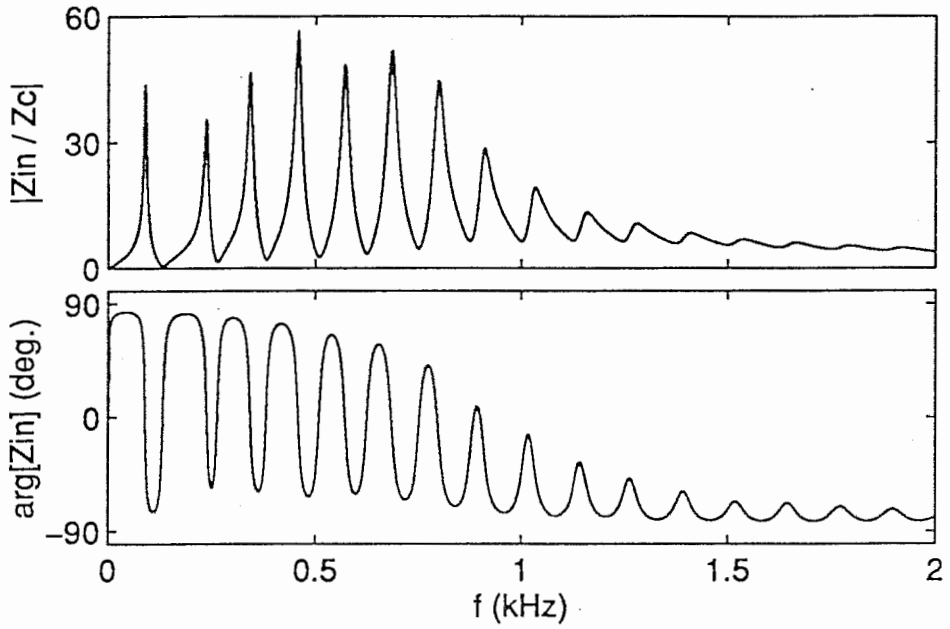

Figure 4

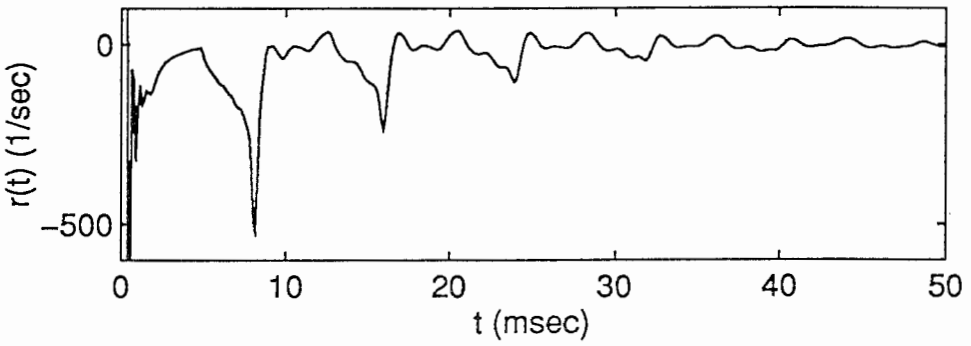

Figure 5

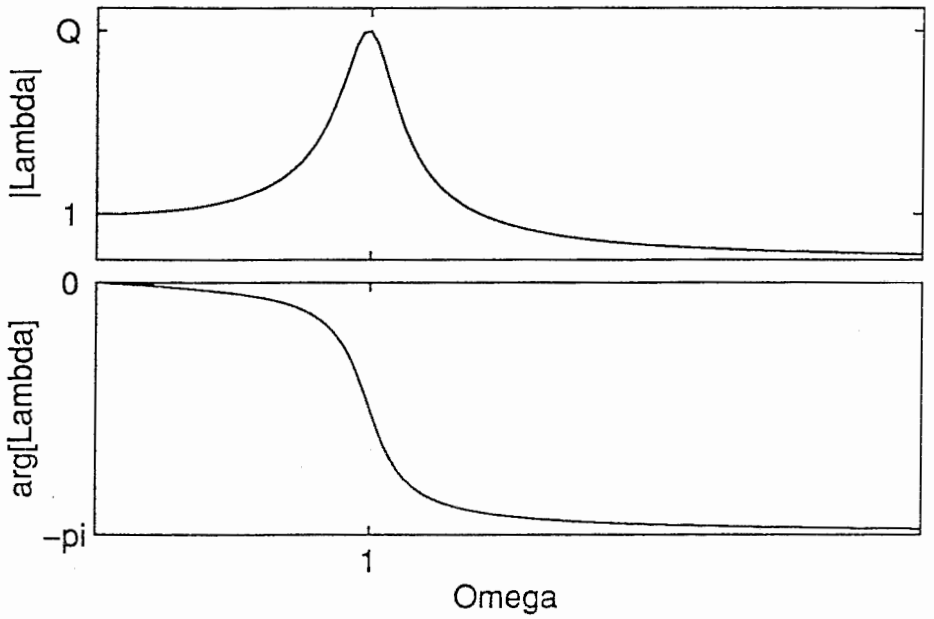

Figure 6

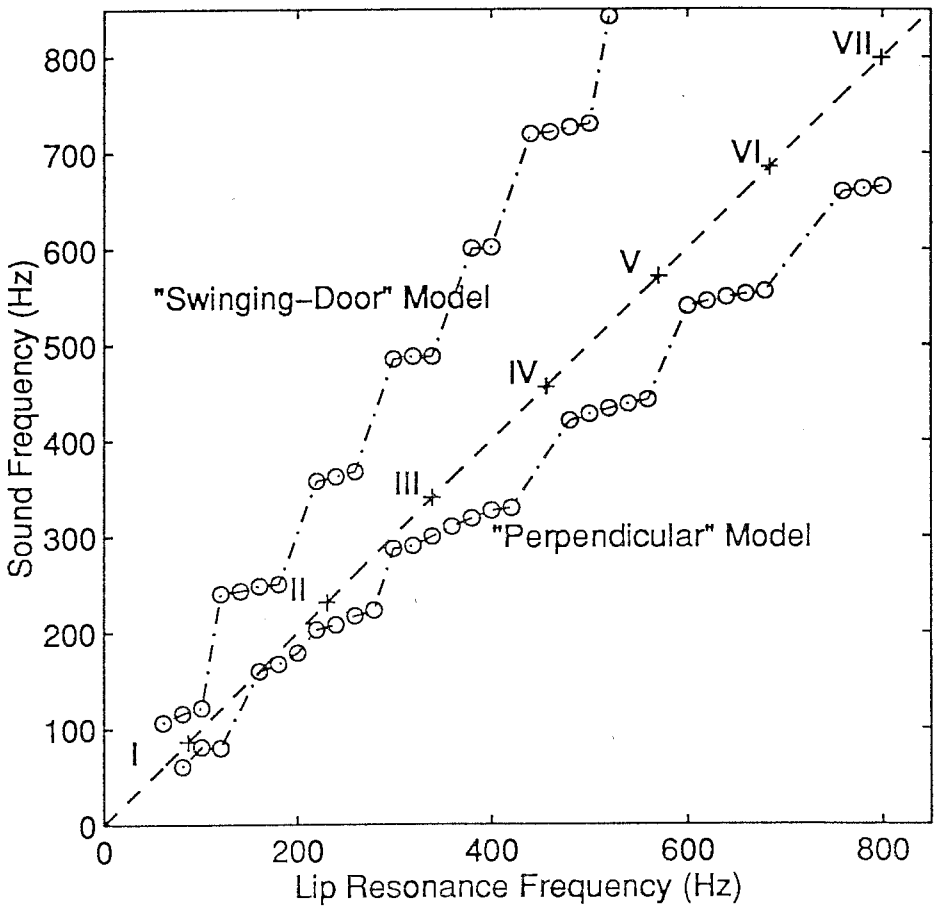
Sound Frequency (Hz)
Lip Resonance Frequency (Hz)
"Swinging–Door" Model
"Perpendicular" Model
I
II
III
IV
V
VI
VII
0
100
200
300
400
500
600
700
800
0
200
400
600
800

Figure 7

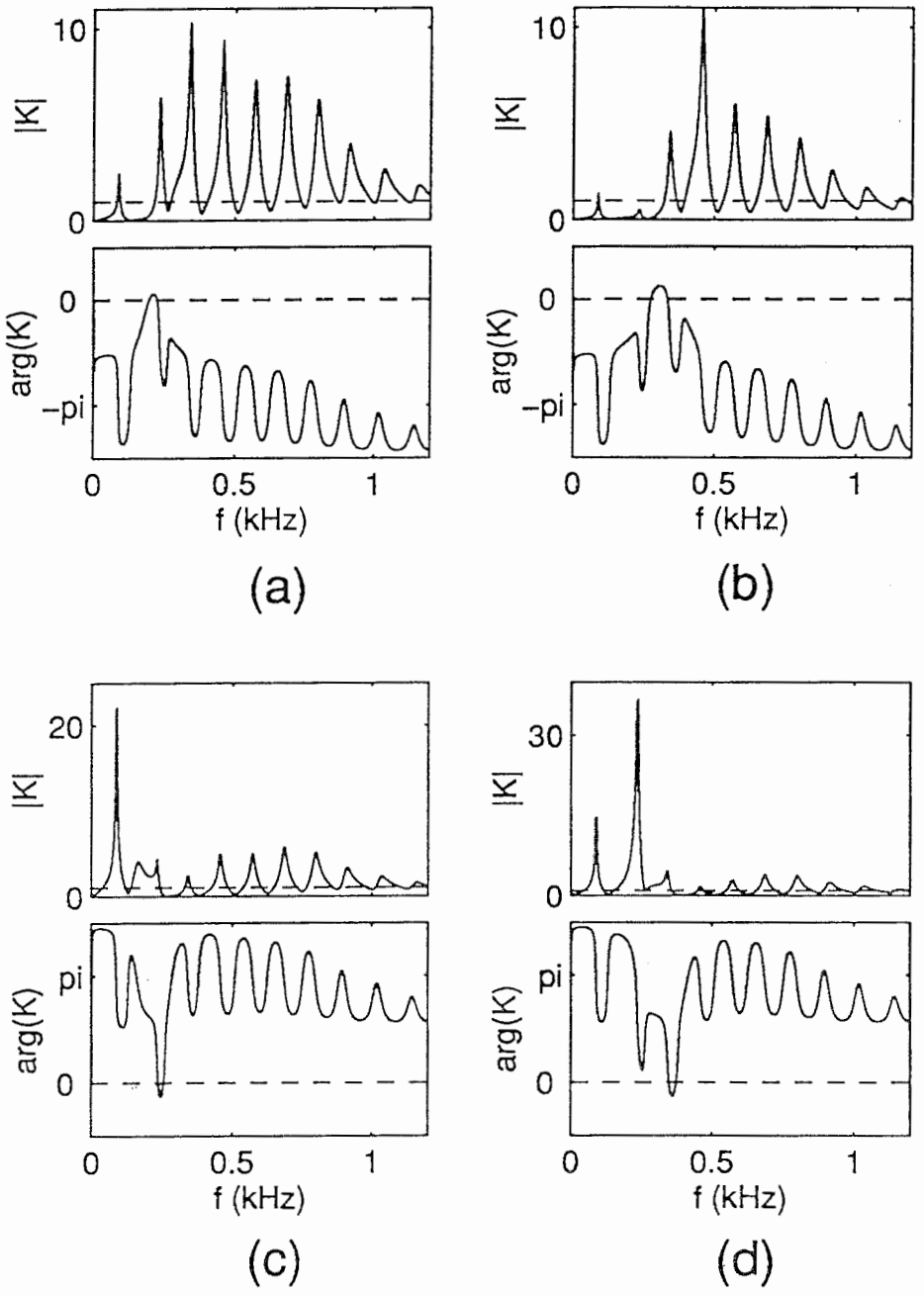
10
|K|
0
arg(K)
0
-pi
0
0.5
1
f (kHz)
(a)
10
|K|
0
arg(K)
0
-pi
0
0.5
1
f (kHz)
(b)
20
|K|
0
arg(K)
pi
0
0
0.5
1
f (kHz)
(c)
30
|K|
0
arg(K)
pi
0
0
0.5
1
f (kHz)
(d)

Figure 8

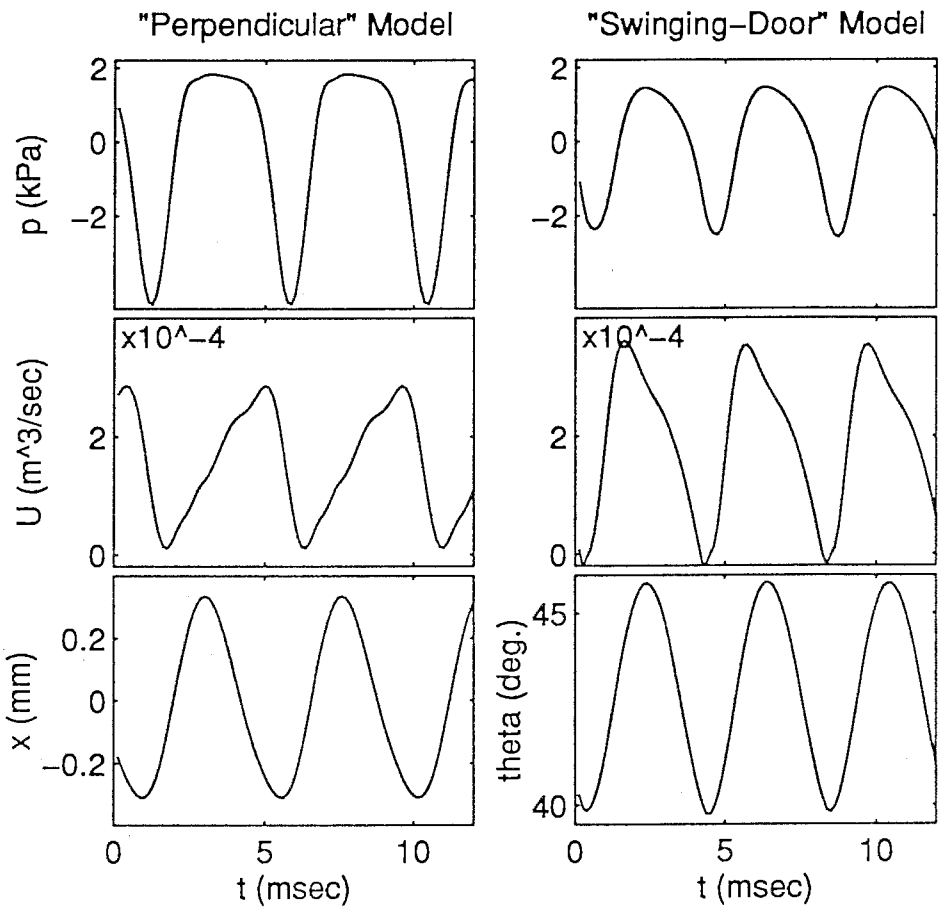
"Perpendicular" Model
"Swinging-Door" Model
p (kPa)
U (m^3/sec)
x (mm)
theta (deg.)
x10^-4
x10^-4
t (msec)
t (msec)

Figure 9

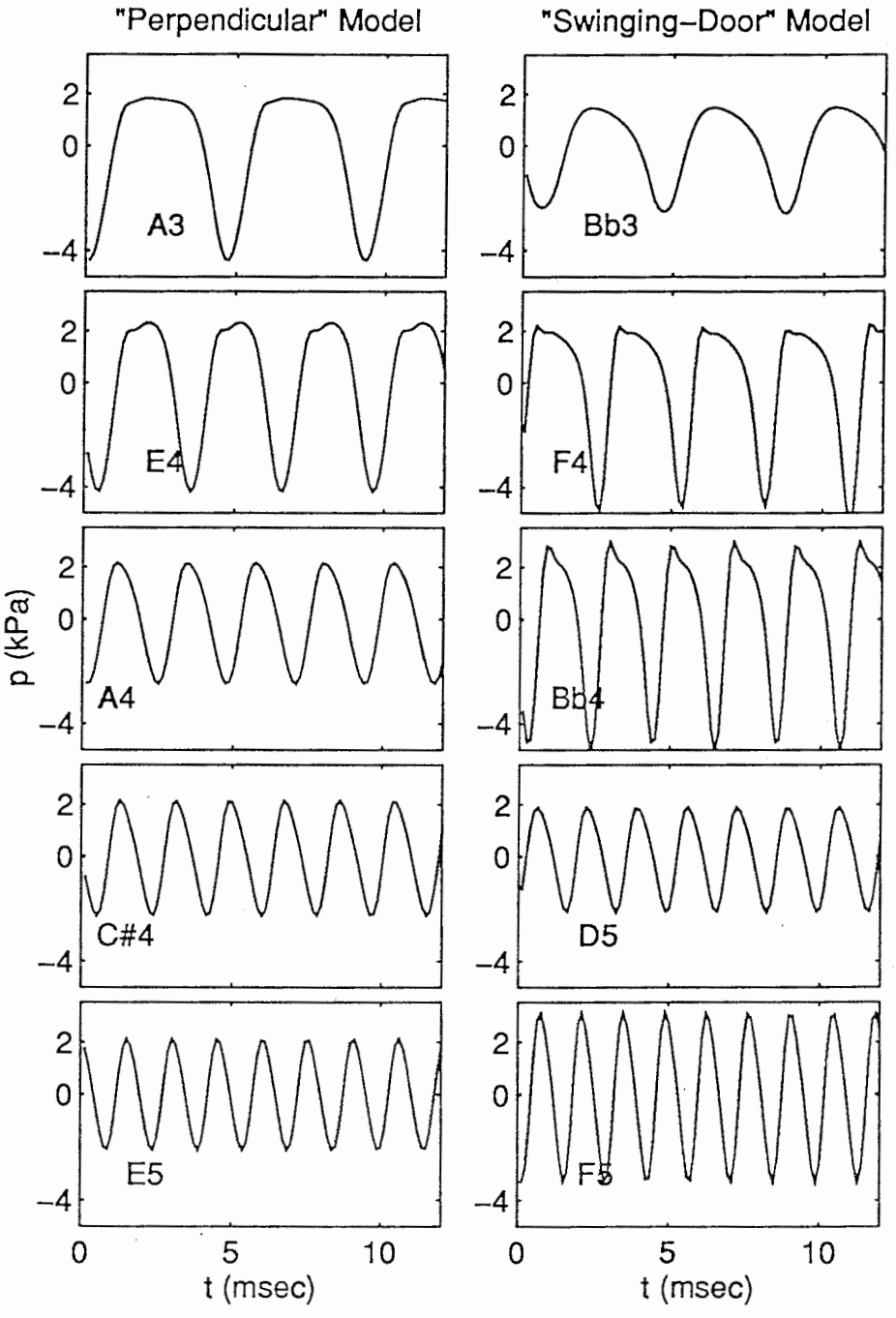
"Perpendicular" Model
"Swinging-Door" Model
A3
Bb3
E4
F4
A4
Bb4
C#4
D5
E5
F5
p (kPa)
t (msec)
t (msec)
2
0
−4
0
5
10

Figure 10

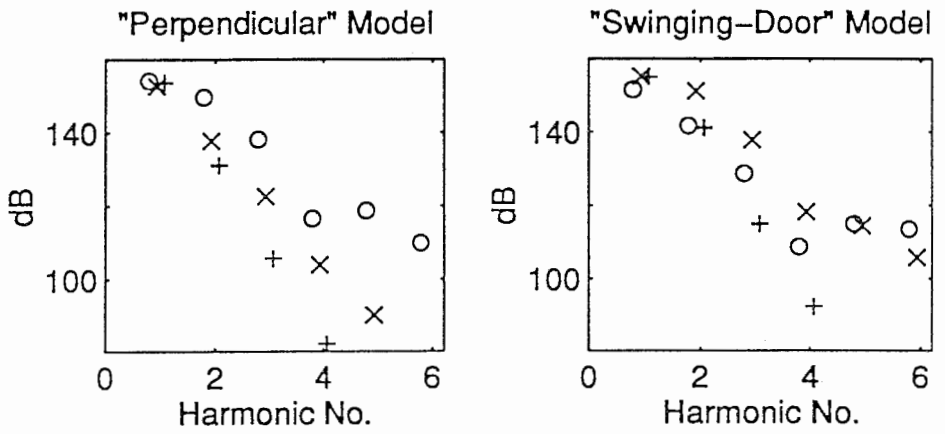
"Perpendicular" Model
"Swinging–Door" Model
dB
140
100
0
2
4
6
Harmonic No.

Figure 11

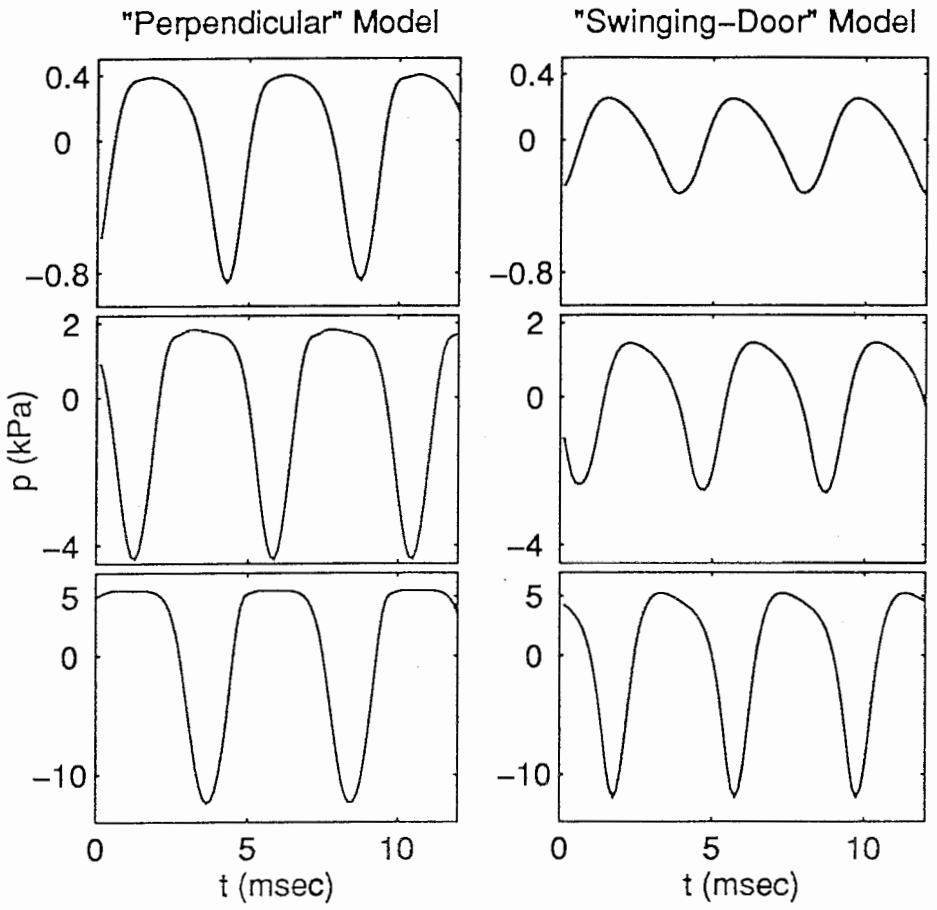
"Perpendicular" Model
"Swinging-Door" Model
0.4
0
-0.8
2
0
-4
5
0
-10
p (kPa)
0
5
10
t (msec)

Figure 12

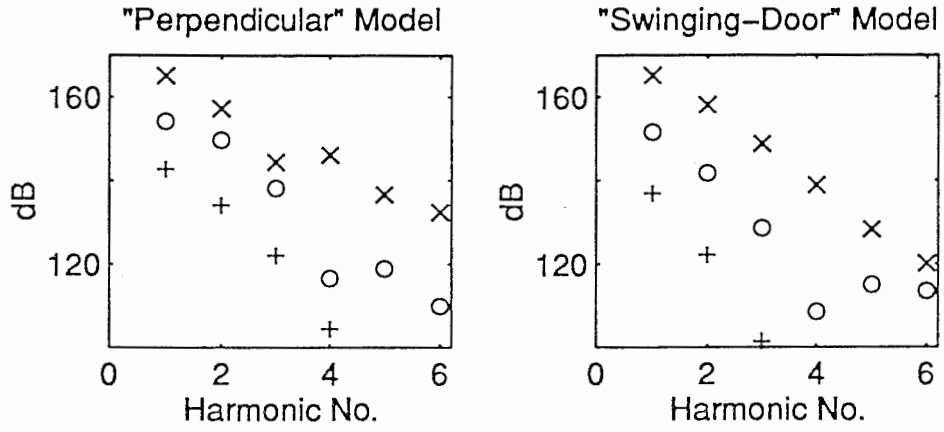
"Perpendicular" Model
"Swinging–Door" Model
dB
160
120
0
2
4
6
Harmonic No.

Figure 13

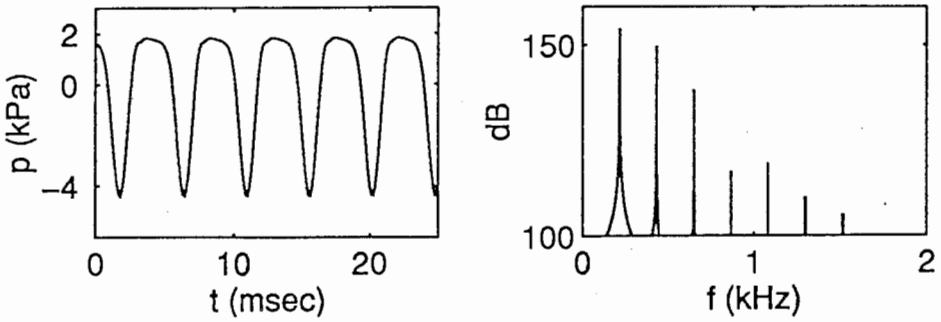

(a)

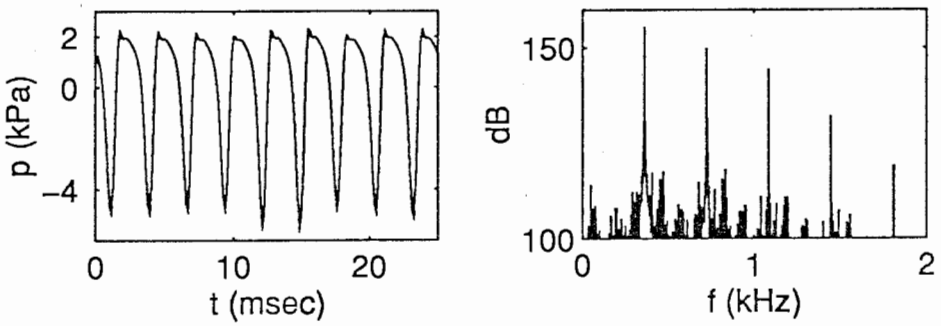

(b)

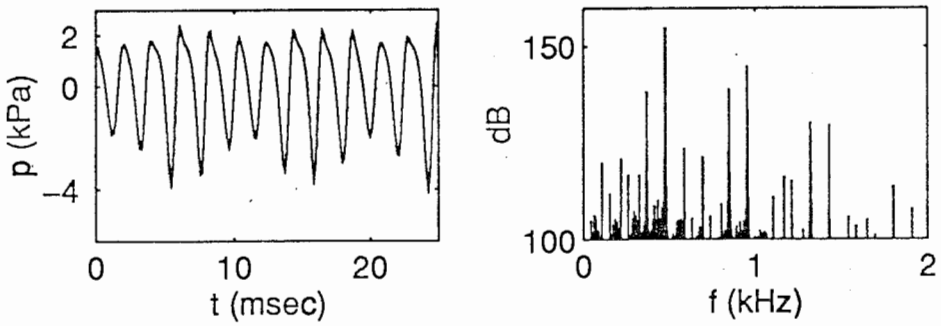

(c)

Figure 14